



This is a repository copy of *Stoichiometrically controlled C-(A)-S-H/N-A-S-H gel blends via alkali activation of synthetic precursors.*

White Rose Research Online URL for this paper:  
<http://eprints.whiterose.ac.uk/164376/>

Version: Accepted Version

---

**Article:**

Walkley, B. [orcid.org/0000-0003-1069-1362](http://orcid.org/0000-0003-1069-1362), Provis, J.L. [orcid.org/0000-0003-3372-8922](http://orcid.org/0000-0003-3372-8922), San Nicolas, R. et al. (2 more authors) (2015) Stoichiometrically controlled C-(A)-S-H/N-A-S-H gel blends via alkali activation of synthetic precursors. *Advances in Applied Ceramics*, 114 (7). pp. 372-377. ISSN 1743-6753

<https://doi.org/10.1179/1743676115Y.0000000057>

---

This is an Accepted Manuscript of an article published by Taylor & Francis in *Advances in Applied Ceramics* on 3rd August 2015, available online:  
<http://www.tandfonline.com/10.1179/1743676115Y.0000000057>.

**Reuse**

Items deposited in White Rose Research Online are protected by copyright, with all rights reserved unless indicated otherwise. They may be downloaded and/or printed for private study, or other acts as permitted by national copyright laws. The publisher or other rights holders may allow further reproduction and re-use of the full text version. This is indicated by the licence information on the White Rose Research Online record for the item.

**Takedown**

If you consider content in White Rose Research Online to be in breach of UK law, please notify us by emailing [eprints@whiterose.ac.uk](mailto:eprints@whiterose.ac.uk) including the URL of the record and the reason for the withdrawal request.



[eprints@whiterose.ac.uk](mailto:eprints@whiterose.ac.uk)  
<https://eprints.whiterose.ac.uk/>

# Stoichiometrically controlled C-(A)-S-H/N-A-S-H gel blends via alkali-activation of synthetic precursors

Brant **Walkley**<sup>1</sup>, John L. **Provis**\*<sup>2</sup>, Rackel **San Nicolas**<sup>3</sup>, Marc-Antoine **Sani**<sup>4</sup>, Jannie S. J. **van Deventer**<sup>5</sup>

<sup>1</sup> Department of Chemical and Biomolecular Engineering, The University of Melbourne, Australia  
b.walkley@student.unimelb.edu.au

<sup>2</sup> Department of Materials Science and Engineering, The University of Sheffield, United Kingdom  
j.provis@sheffield.ac.uk

<sup>3</sup> Department of Infrastructure Engineering, The University of Melbourne, Australia  
rackel.san@unimelb.edu.au

<sup>4</sup> Department of Chemistry and Bio21 Institute, The University of Melbourne, Australia  
msani@unimelb.edu.au

<sup>5</sup> Zeobond Pty Ltd, P.O Box 23450, Docklands, Victoria, Australia  
jannie@zeobond.com

\*Corresponding author: J. L. Provis, j.provis@sheffield.ac.uk, +44 114 222 5490, Department of Materials Science and Engineering, The University of Sheffield, Sheffield S1 3JD, United Kingdom

## Abstract

The extent to which the composition of the reaction mix affects the formation of a biphasic C-(A)-S-H/N-A-S-H geopolymer framework, and how the interaction of these phases affects geopolymer microstructure, can only be studied by strict stoichiometric control. Stoichiometrically controlled geopolymers containing both C-(A)-S-H and N-A-S-H gels are produced here by reaction of a sodium silicate solution with calcium-aluminosilicate powders, which were synthesised via a novel solution-polymerisation method utilising polyethylene glycol as a polymer carrier to sterically inhibit movement of precursor cations. Increased Ca content in the reaction mix appears to promote greater formation of a C-(N)-(A)-S-H gel, while reduced Ca content and increased Al and Si content promote greater formation of an N-A-S-H gel in addition to the main C-(A)-S-H reaction product. The stoichiometrically controlled geopolymers constitute a chemically simplified model system through which the nature of the biphasic C-(A)-S-H/N-A-S-H gels present in alkali activated binders can be studied.

**Keywords:** Geopolymer, alkali-activated binders, aluminosilicate powder synthesis, NMR spectroscopy

## 1. Introduction

Geopolymers and alkali-activated binders offer a viable low-CO<sub>2</sub> alternative to ordinary Portland cement (OPC) and exhibit desirable technical properties, as well as a potential reduction in CO<sub>2</sub> emissions by over 80%<sup>1-3</sup>. Industrial by-products such as fly ash and granulated blast furnace slag are often used as raw materials for the production of geopolymers and alkali-activated binders, and the chemical composition of these materials varies significantly between sources<sup>2, 4</sup>. Variations in the composition of the raw material can significantly affect the technical properties exhibited by these binders, and as such there is currently no single formulation that can be used to produce geopolymers and alkali-activated binders which possess similar physical and chemical characteristics across a wide range of precursor compositions<sup>2, 4</sup>.

Coexistence of both C-(A)-S-H and N-A-S-H gel frameworks within alkali-activated binders results in complex thermodynamic and chemical interactions, which dictate material properties and performance. Despite the vast number of studies investigating the chemistry of alkali-activated binders, the literature is often conflicting and the experimental analysis involves a large number of unconstrained parameters. This is, at least in part, due to the production of alkali-activated binders using raw materials which display large variations in chemical and mineralogical composition. It is therefore necessary to develop a method to study alkali-activated binders with strict control of the stoichiometry in these systems, to gain a more complete understanding of the relationships between thermodynamics, reaction kinetics and the initial compositions of the precursors used to produce alkali-activated materials.

Sol-gel based procedures<sup>5</sup> have been used to synthesise and investigate the effect of composition on C-(A)-S-H and N-A-S-H phase assemblages<sup>6-10</sup> in the past, as well as to conduct compatibility studies of C-S-H and N-A-S-H gels<sup>8, 10</sup>. However, these studies mostly investigate the effect of addition of alkali cations, alkaline earth cations or aluminium on the properties of C-S-H or N-A-S-H gels after formation of the gel. In order to accurately represent the physical and chemical interactions occurring during the actual process of alkali-activation, all of the ionic species of interest must be present in a precursor powder prior to alkali-activation.

This study examines the effect of precursor material composition on C-(A)-S-H and N-A-S-H phase assemblage by synthesising calcium, silicon and aluminium containing mixed oxides via an organic polymeric steric entrapment solution-polymerisation route<sup>11</sup>. This method utilises polyethylene glycol (PEG) to sterically inhibit the movement of the metal cations during solution-polymerisation, forming a homogeneous mixed oxide powder upon drying. The stoichiometrically controlled reactive precursor powders are subsequently activated with an alkaline solution to form an alkali-activated binder. The effects of the Ca, Si and Al in the reaction mix on the chemistry and microstructure of the geopolymer binder are assessed here by electron microscopy, X-ray diffraction and nuclear magnetic resonance (NMR) spectroscopy.

## 2. Experimental Methods

### 2.1 Precursor powder synthesis

A 5 wt.% polyethylene glycol (PEG) solution was made by adding polyethylene glycol powder (Sigma Aldrich, molecular weight 20 kDa) to distilled water and stirring at 60°C. Aluminium nitrate nonahydrate, Al(NO<sub>3</sub>)<sub>3</sub>·9H<sub>2</sub>O (Sigma Aldrich, 98.5 wt.%), and calcium nitrate tetrahydrate, Ca(NO<sub>3</sub>)<sub>2</sub>·4H<sub>2</sub>O (Sigma Aldrich), were added to distilled water to produce 40 wt.% solutions of each, which were then added to the 5 wt.% solution of polyethylene glycol and stirred at 60°C.

Colloidal silica, SiO<sub>2</sub> (Sigma Aldrich, 40 wt.% in water), was added to the 5 wt.% solution of polyethylene glycol containing aqueous aluminium and calcium nitrates, and water was evaporated by stirring over heat at 80°C to form a viscous aerated gel. The stoichiometry of the metal cation-polyethylene glycol solution was designed so that the ratio of positive valences from the metal cations to negative valences from the polymer was 2.0. The viscous aerated gel was then placed in a drying oven at 100°C overnight. The dry polymer matrix was then calcined at 900°C to produce a fine white powder which was subsequently ground by hand using a mortar and pestle in preparation for characterisation and alkali-activated binder synthesis.

## 2.2 Alkali-activated binder synthesis

The activating solution was prepared by dissolution of sodium hydroxide powder (AnalaR, 99 wt.%) in sodium silicate solution (N grade, 37.5 wt.%, PQ Australia) and distilled water. The reaction mixtures had an activating solution modulus of SiO<sub>2</sub>/Na<sub>2</sub>O = 1, a water/solids ratio of 0.75 and cation ratios as outlined in Table 1. The activating solution was mixed with the precursor powder to form a homogeneous paste, which was subsequently cast in sealed containers and cured at ambient temperature for 3 and 28 days.

**Table 1.** Molar ratios of the reaction mix for each sample

Sample	Ca/(Al+Si)	Al/Si	Na/Al
A	0.67	0.15	0.5
B	1.00	0.15	0.5

## 2.3 Characterisation

X-ray diffraction (XRD) data were collected using a Bruker D8 Advance instrument with Cu K $\alpha$  radiation, a nickel filter, a step size of 0.020°, and a counting time of 3 s/step. Environmental scanning electron microscopy (ESEM) was conducted using an FEI Quanta instrument with a 15 kV accelerating voltage, a working distance of 10.0 mm and a Link-Isis (Oxford) X-ray energy dispersive (EDX) detector. <sup>29</sup>Si magic angle spinning (MAS) NMR spectra were collected at 119.141 MHz on an Agilent (Varian) VNMRS-600 (14.1 T) instrument with a pulse width of 7  $\mu$ s, a relaxation delay of 120 s and 1024 scans. <sup>27</sup>Al MAS NMR spectra were acquired on the same instrument at 156.261 MHz, with a pulse width of 4  $\mu$ s, a relaxation delay of 2 s and 1024 scans.

## 3. Results and discussion

### 3.1 X-Ray diffraction

X-ray diffractograms of the calcined precursor powder and the alkali-activated binders are presented in Fig. 1. The X-ray diffractograms of the calcined precursor powders display two broad, featureless humps centred at  $\sim 14^\circ 2\theta$  and  $\sim 30^\circ 2\theta$ , indicating a predominantly amorphous material. Small amounts of tricalcium aluminate (C<sub>3</sub>A; PDF # 33-0251) and two polymorphs of dicalcium silicate (C<sub>2</sub>S; PDF # 33-0302 and 36-0642) are identified in the calcined precursor powder of both samples, while a small amount of crystalline calcium oxide (PDF # 48-1467) is also identified in the calcined precursor powder of sample B. Calcination of the precursor powder to 900°C is necessary to remove any calcium carbonate present in the sample (converting it to free lime), however it is evident from the X-ray diffractograms in Fig. 1 that the calcination process has caused some devitrification of the amorphous material and subsequent formation of a small amount of these crystalline phases. Alkali-activation of both samples A and B produces a much

broader amorphous hump centred at approximately  $29^\circ 2\theta$ , characteristic of alkali-activated materials and indicative of the formation of a predominantly amorphous reaction product consistent with that formed during alkali-activation of granulated blast furnace slag<sup>12, 13</sup>. The main reaction product in both samples is a poorly crystalline aluminium-substituted calcium silicate hydrate (C-(A)-S-H) phase with structural similarity to aluminium-containing tobermorite (PDF # 19-0052).

In both samples the crystalline phases present in the calcined precursor powder are partially consumed during alkali activation, leading to the formation of poorly ordered C-(A)-S-H and crystalline  $C_4AH_{13}$  (PDF # 02-0077).  $C_2S$  is progressively consumed as the alkali-activation reaction continues. Small amounts of stilbite-Ca ( $NaCa_2Al_5Si_{13}O_{36} \cdot 14H_2O$ ) (PDF # 44-1479) are evident in the alkali-activated binders cured for 3 and 28 days for sample A, while the diffractograms of the alkali-activated binder cured for 3 and 28 days for sample B indicate the presence of portlandite ( $Ca(OH)_2$ ) (PDF # 44-1481) which is likely to have, in part, formed as a result of dissolution and hydration of  $C_2S$ . A partially silicate-substituted AFm phase ( $[Ca_2Al(OH)_6] \cdot X \cdot xH_2O$  where X is a doubly charged carbonate or aluminosilicate anion) is also observed in both samples<sup>14, 15</sup>. Increased calcium content in the precursor powder appears to promote the formation of portlandite in addition to the main C-(A)-S-H and  $C_4AH_{13}$  products.

### 3.2 Scanning electron microscopy

The compositions of the alkali-activated binders for samples A and B as determined by ESEM – EDX are reported in Fig. 2. The chemistry of both alkali-activated binders differs from that of the reaction mix. The Ca/(Al+Si) ratio of the alkali-activated binder for sample A is lower than that of the reaction mix, while the alkali-activated binder of sample B is more Ca-rich and Si-deficient than the reaction mix, with a slight increase in Al content. It is also clear that Na has been incorporated into the binder for both samples, likely assuming a charge balancing function within a sodium and aluminium substituted calcium silicate hydrate (C-(N)-(A)-S-H) gel. Values for the Ca/(Al+Si) ratio exhibited by the alkali-activated binder for sample B lie along a line which can be drawn between the Ca/(Al+Si) ratios of a C-(A)-S-H gel and a partially silicate-substituted AFm phase. This is likely to be a result of intermixing of the C-(A)-S-H gel and AFm and portlandite phases. The lower Ca content in the reaction mix for sample A seems to promote the formation of a C-(N)-(A)-S-H gel, whereas the higher content of Ca in the reaction mix for sample B appears to promote formation of a C-(A)-S-H gel<sup>10</sup>.

The compositional range for single phase C-(A)-S-H, as determined by experimental observation<sup>16, 17</sup> and thermodynamic modeling<sup>18</sup>, is less extensive than the values observed for the alkali-activated binders in Fig. 2. As such it is likely that the chemistry of the alkali-activated binders for samples A and B is a combination of the chemistry of both highly crosslinked framework silicate (N-A-S-H) and chain silicate (C-(N)-(A)-S-H or C-A-S-H) gel structures, as well as contributions from the portlandite and AFm phases identified by XRD. This suggests that the lower Ca content in the reaction mix for sample A is promoting the formation of a sodium aluminium silicate hydrate (N-A-S-H) gel in addition to the C-(N)-(A)-S-H gel, whereas the higher content of Ca in the reaction mix for sample B promotes greater inclusion of Al in the C-(N)-(A)-S-H binder. The main reaction product will be a mixture of C-(N)-(A)-S-H and N-A-S-H gels<sup>18</sup>, however lower levels of Ca in the reaction mix will drive the substitution of Al to form a C-A-S-H gel, as well as incorporation of Na to form a C-(N)-(A)-S-H gel, and this will progress to a point which achieves the maximum Al and Na incorporation that is thermodynamically stable. The decreased Ca/(Al+Si) ratio in the reaction mix

of sample A will drive increased formation of N-A-S-H. Higher concentrations of Ca in the initial reaction mix (as is the case for sample B) will drive further development of C-(N)-(A)-S-H.

### 3.3 Nuclear magnetic resonance spectroscopy

$^{27}\text{Al}$  MAS NMR spectra for the calcined precursor powders and alkali-activated binders are presented in Fig. 3. The spectra of the two calcined precursor powders are very similar, displaying a broad tetrahedral Al resonance centred at approximately 54 and 56 ppm for samples A and B, respectively. The breadth of this resonance indicates that there is a distribution of Al environments in each sample, rather than a single well defined site. This resonance is attributed to the glassy phase responsible for the broad amorphous hump in the X-ray diffractograms of the uncalcined precursor powders, and is similar to that observed for granulated blast furnace slag<sup>12, 13</sup>. Both samples A and B display a low intensity broad resonance centred at approximately 0 ppm, partly overlapping the downfield spinning side band of the main Al(IV) peak, attributed to octahedral Al. This is consistent with the small amount of  $\text{C}_3\text{A}$  identified by XRD in both calcined precursor powders.

The  $^{27}\text{Al}$  MAS NMR spectra of the alkali-activated binders for both samples A and B display a low intensity broad resonance from 30 ppm to 70 ppm centred at approximately 55 ppm and again assigned to Al in a significantly distorted tetrahedral environment, as well as a low intensity narrow resonance at approximately 72 ppm assigned to Al in a well defined tetrahedral coordination and a high intensity narrow resonance at approximately 6.5 ppm assigned to Al in a well defined octahedral coordination. A small contribution to the resonance at 72 ppm is also expected from a spinning side band of the sharp resonance at 6.5 ppm, as indicated in Fig.3. Ordered C-(A)-S-H identified in the alkali-activated binders for both samples by XRD will contain Al substituted for Si in a tetrahedrally coordinated environment, leading to the well defined resonance observed at 72 ppm, while poorly crystalline C-(A)-S-H and N-A-S-H will each contain Al in significantly distorted tetrahedral environments, leading to the broad resonance observed between 30 ppm to 70 ppm and centred at approximately 55 ppm. The secondary reaction product  $\text{C}_4\text{AH}_{13}$  is responsible for the well defined resonance observed at 6.5 ppm<sup>19</sup>.

$^{29}\text{Si}$  MAS NMR spectra of the calcined precursor powders and alkali-activated binders are presented in Fig. 4. For both samples A and B the spectra of the calcined aluminosilicate powder display a broad resonance centred at approximately -82 ppm. Due to its broad nature it is likely this resonance contains contributions from each of the  $\text{Q}^1$ ,  $\text{Q}^2$  and  $\text{Q}^2(1\text{Al})$  lower connectivity silicon environments as well as highly Al-substituted  $\text{Q}^4$  silicon coordination environments<sup>12</sup>. Alkali-activation of the calcined precursor powder for sample A causes a significant reduction in the intensity of the  $\text{Q}^1$  region of the spectra and a significant increase in intensity at -81 ppm and -84 ppm. This region is assigned to  $\text{Q}^2$  and  $\text{Q}^2(1\text{Al})$  environments, indicating the formation of a C-(A)-S-H gel<sup>12</sup>. A significant increase in intensity is observed within the -90 to -100 ppm region of the spectra commonly assigned to aluminium-substituted  $\text{Q}^3$  and  $\text{Q}^4$  species, suggesting the formation of a N-A-S-H gel, with some contribution to this resonance expected from the aluminosilicate anion present in the AFm secondary reaction product as observed by XRD.

Similarly, upon alkali-activation sample B displays a significant reduction in the intensity of the  $\text{Q}^1$  region of the spectra, as well as a slight reduction in intensity in the Al substituted  $\text{Q}^4$  region of the spectra, and a significant increase in the intensity at -81 ppm and -84 ppm. This increase is again assigned to formation of  $\text{Q}^2$  and  $\text{Q}^2(1\text{Al})$  environments present in a C-(A)-S-H gel. The increased intensity of the resonance assigned to  $\text{Q}^3$  species upon alkali-activation of sample A suggests that a

lower Ca content in the reaction mix promotes formation of a N-A-S-H gel in addition to the main C-(A)-S-H reaction product, while higher Ca content in the reaction mix promotes greater formation of the C-(A)-S-H reaction product. This is in agreement with the ESEM-EDX observations (Fig. 2) that the alkali-activated binder of sample B is more Al-rich than the bulk chemistry of the reaction mix.

#### 4. Conclusions

Stoichiometrically controlled alkali-activated binders were synthesised via alkali-activation of calcium-aluminosilicate precursor powders. These precursor powders were synthesised from aqueous precursor solutions via an organic steric entrapment solution-polymerisation route utilising polyethylene glycol to sterically inhibit the movement of precursor cations. The main reaction product in both samples was a biphasic C-(A)-S-H/N-A-SH gel. Increased Ca content within the reaction mix appears to promote greater formation of C-(N)-(A)-S-H, while reduced Ca content and increased Al and Si content in the reaction mix appear to promote greater formation of N-A-S-H in addition to the main C-(A)-S-H reaction product. The stoichiometrically controlled alkali-activated binders constitute a chemically simplified model system through which the nature of the biphasic C-(A)-S-H/N-A-S-H gels present in alkali-activated binders can be studied.

#### Acknowledgements

This work was funded in part by the Australian Research Council (ARC), including support through the Particulate Fluids Processing Centre, a Special Research Centre of the ARC, and through an Australian Postgraduate Award supporting the doctoral studies of BW.

#### References

1. J. Davidovits: 'Geopolymers - Inorganic polymeric new materials', *Journal of Thermal Analysis*, 1991, **37**(8), 1633-1656.
2. P. Duxson, J. L. Provis, G. C. Lukey, and J. S. J. van Deventer: 'The role of inorganic polymer technology in the development of 'green concrete'', *Cement and Concrete Research*, 2007, **37**(12), 1590-1597.
3. M. C. G. Juenger, F. Winnefeld, J. L. Provis, and J. H. Ideker: 'Advances in alternative cementitious binders', *Cement and Concrete Research*, 2011, **41**(12), 1232-1243.
4. P. Duxson, A. Fernandez-Jimenez, J. L. Provis, G. C. Lukey, A. Palomo, and J. S. J. van Deventer: 'Geopolymer technology: the current state of the art', *Journal of Materials Science*, 2007, **42**(9), 2917-2933.
5. R. K. Iler: 'The chemistry of silica : solubility, polymerization, colloid and surface properties, and biochemistry', 1979, New York, Wiley.
6. X.-m. Cui, L.-p. Liu, G.-j. Zheng, R.-p. Wang, and J.-p. Lu: 'Characterization of chemosynthetic  $\text{Al}_2\text{O}_3$ - $2\text{SiO}_2$  geopolymers', *Journal of Non-Crystalline Solids*, 2010, **356**(2), 72-76.
7. G. Zheng, X. Cui, W. Zhang, and Z. Tong: 'Preparation of geopolymer precursors by sol-gel method and their characterization', *Journal of Materials Science*, 2009, **44**(15), 3991-3996.
8. I. García-Lodeiro, A. Fernández-Jiménez, M. T. Blanco, and A. Palomo: 'FTIR study of the sol-gel synthesis of cementitious gels: C-S-H and N-A-S-H', *Journal of Sol-Gel Science and Technology*, 2008, **45**(1), 63-72.
9. I. García-Lodeiro, A. Fernández-Jiménez, A. Palomo, and D. E. Macphee: 'Effect of calcium additions on N-A-S-H cementitious gels', *Journal of the American Ceramic Society*, 2010, **93**(7), 1934-1940.
10. I. Garcia-Lodeiro, A. Palomo, A. Fernández-Jiménez, and D. E. Macphee: 'Compatibility studies between N-A-S-H and C-A-S-H gels. Study in the ternary diagram  $\text{Na}_2\text{O}$ - $\text{CaO}$ - $\text{Al}_2\text{O}_3$ - $\text{SiO}_2$ - $\text{H}_2\text{O}$ ', *Cement and Concrete Research*, 2011, **41**(9), 923-931.
11. M. A. Gulgun, M. H. Nguyen, and W. M. Kriven: 'Polymerized organic-inorganic synthesis of mixed oxides', *Journal of the American Ceramic Society*, 1999, **82**(3), 556-560.
12. S. A. Bernal, J. L. Provis, B. Walkley, R. San Nicolas, J. D. Gehman, D. G. Brice, A. R. Kilcullen, P. Duxson, and J. S. J. van Deventer: 'Gel nanostructure in alkali-activated binders based on slag and fly ash, and effects of accelerated carbonation', *Cement and Concrete Research*, 2013, **53**, 127-144.

13. S. A. Bernal, R. San Nicolas, R. J. Myers, R. Mejía de Gutiérrez, F. Puertas, J. S. J. van Deventer, and J. L. Provis: 'MgO content of slag controls phase evolution and structural changes induced by accelerated carbonation in alkali-activated binders', *Cement and Concrete Research*, 2014, **57**, 33-43.
14. B. Lothenbach, G. Le Saout, E. Gallucci, and K. Scrivener: 'Influence of limestone on the hydration of Portland cements', *Cement and Concrete Research*, 2008, **38**(6), 848-860.
15. T. Matschei, B. Lothenbach, and F. P. Glasser: 'The AFm phase in Portland cement', *Cement and Concrete Research*, 2007, **37**(2), 118-130.
16. J. S. J. van Deventer, R. San Nicolas, I. Ismail, S. A. Bernal, D. G. Brice, and J. L. Provis: 'Microstructure and durability of alkali-activated materials as key parameters for standardization', *Journal of Sustainable Cement-Based Materials*, 2015, **4**, 116-128.
17. X. Parda, I. Pochard, and A. Nonat: 'Experimental study of Si–Al substitution in calcium-silicate-hydrate (C-S-H) prepared under equilibrium conditions', *Cement and Concrete Research*, 2009, **39**(8), 637-643.
18. R. J. Myers, S. A. Bernal, R. San Nicolas, and J. L. Provis: 'Generalized structural description of calcium-sodium aluminosilicate hydrate gels: the cross-linked substituted tobermorite model', *Langmuir*, 2013, **29**(17), 5294-5306.
19. P. Pena, J. M. Rivas Mercury, A. H. de Aza, X. Turrillas, I. Sobrados, and J. Sanz: 'Solid-state  $^{27}\text{Al}$  and  $^{29}\text{Si}$  NMR characterization of hydrates formed in calcium aluminate–silica fume mixtures', *Journal of Solid State Chemistry*, 2008, **181**(8), 1744-1752.

**List of figure-captions (low-resolution image included)**

CSH – calcium silicate hydrate C<sub>2</sub>S – dicalcium silicate C<sub>4</sub>AH<sub>13</sub> – hydroxyl-AFm C – calcium oxide  
 C<sub>3</sub>A – tricalcium aluminate ST – stilbite-Ca P - portlandite AFm – silicate-substituted AFm

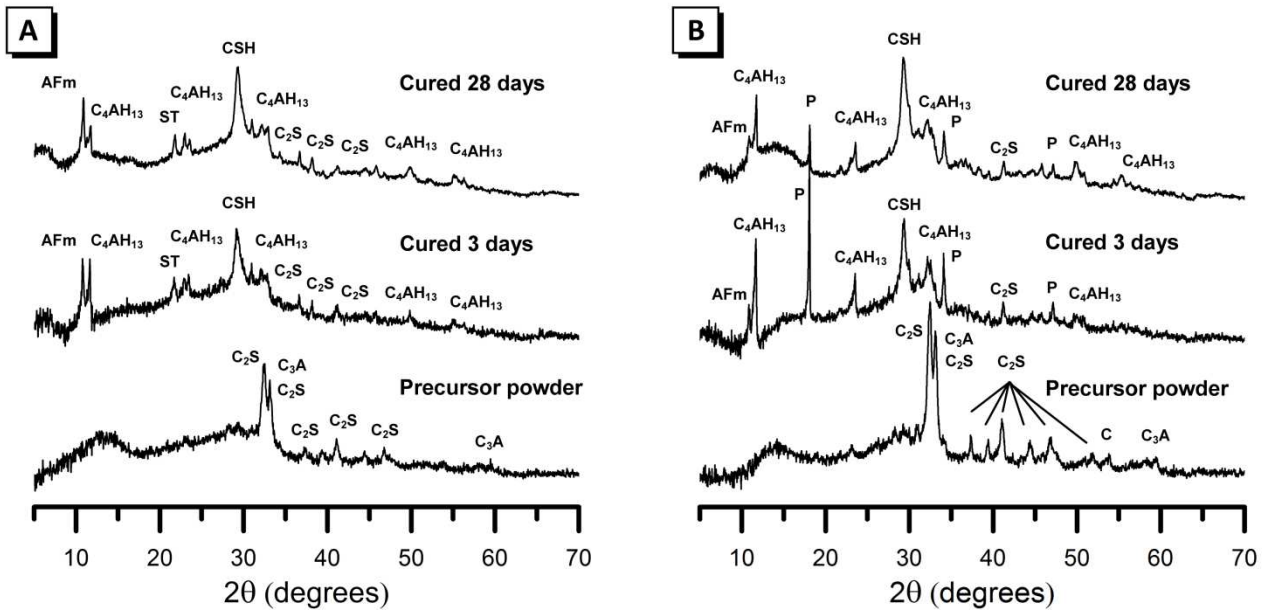


**Figure 1.** X-ray diffractograms of the calcined precursor powder, and alkali-activated binders cured for 3 days and 28 days, for samples A and B as marked.

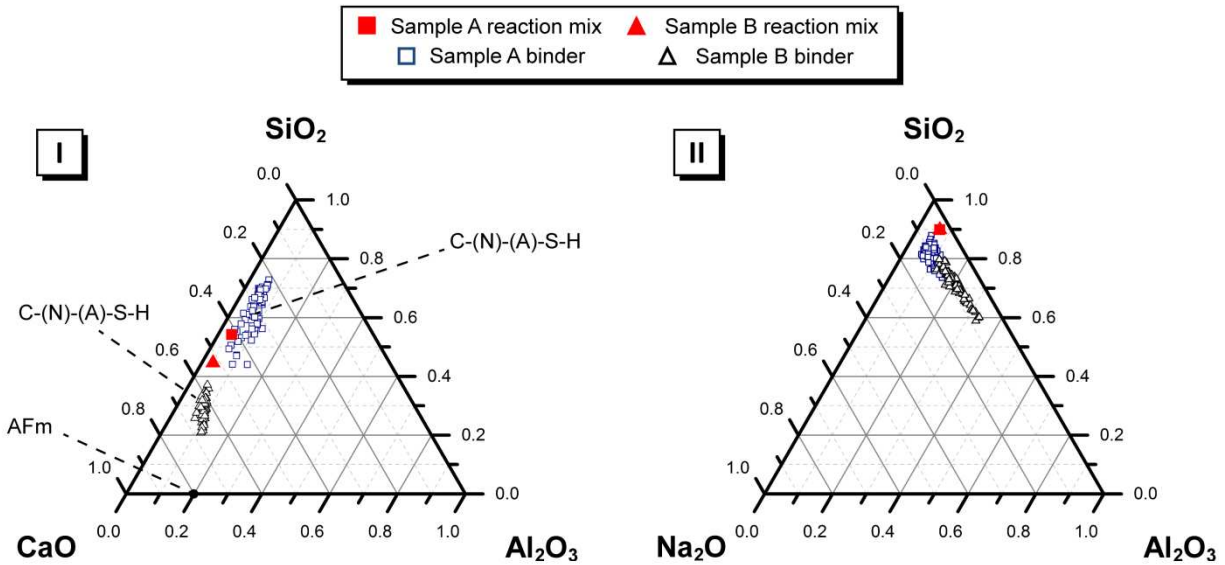


**Figure 2.** Projection of alkali-activated binder chemistry onto the (I) ternary CaO – Al<sub>2</sub>O<sub>3</sub> – SiO<sub>2</sub> system (neglecting Na<sub>2</sub>O content) and (II) ternary Na<sub>2</sub>O – Al<sub>2</sub>O<sub>3</sub> – SiO<sub>2</sub> system (neglecting CaO content) showing elemental composition of alkali-activated binders cured for 3 days for samples A and B as determined by ESEM-EDX analysis.

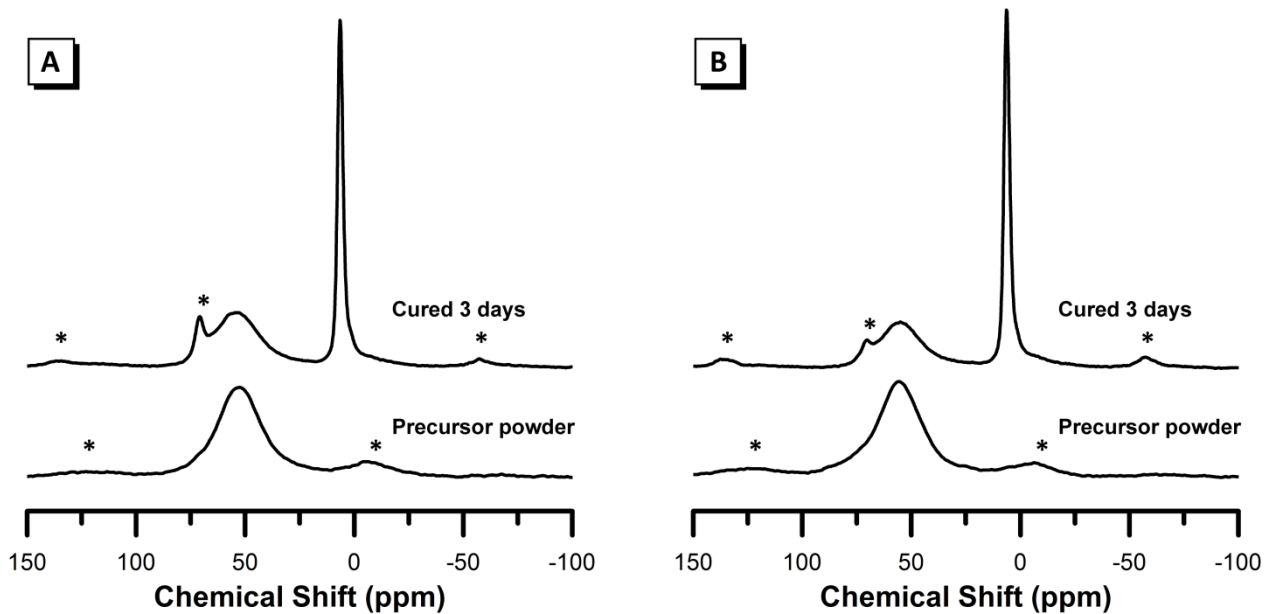


**Figure 3.**  $^{27}\text{Al}$  MAS NMR spectra of (A) sample A and (B) sample B. The expected position of spinning side bands are indicated by \*.

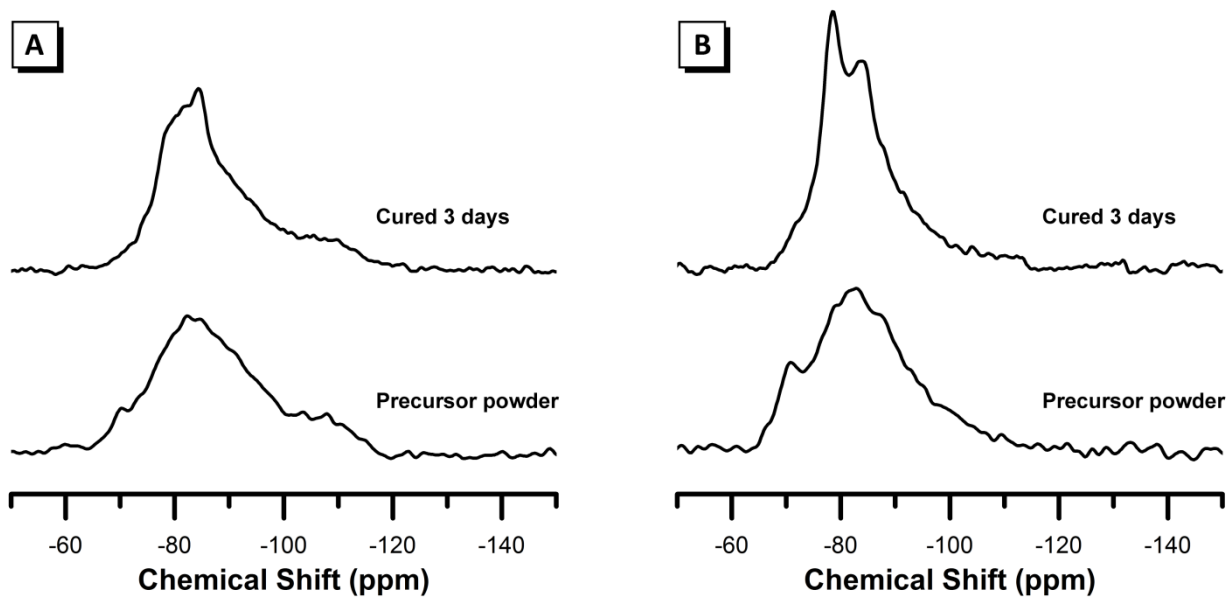


**Figure 4.**  $^{29}\text{Si}$  MAS NMR spectra of (A) sample A and (B) sample B.